Science Bulletin 66 (2021) 1917–1924

Contents lists available at ScienceDirect

Science Bulletin

journal homepage: www.elsevier.com/locate/scib

Article

Aerosol as a critical factor causing forecast biases of air temperature in global numerical weather prediction models

Xin Huang [a,b], Aijun Ding [a,b,*]

[a] School of Atmospheric Sciences, Nanjing University, Nanjing 210023, China
[b] Jiangsu Provincial Collaborative Innovation Center of Climate Change, Nanjing 210023, China

ARTICLE INFO

Article history:
Received 9 December 2020
Received in revised form 13 March 2021
Accepted 19 March 2021
Available online 14 May 2021

Keywords:
Weather prediction
Atmospheric aerosol
Temperature forecast errors
Aerosol–radiation interactions
Aerosol–cloud interactions

ABSTRACT

Weather prediction is essential to the daily life of human beings. Current numerical weather prediction models such as the Global Forecast System (GFS) are still subject to substantial forecast biases and rarely consider the impact of atmospheric aerosol, despite the consensus that aerosol is one of the most important sources of uncertainty in the climate system. Here we demonstrate that atmospheric aerosol is one of the important drivers biasing daily temperature prediction. By comparing observations and the GFS prediction, we find that the monthly-averaged bias in the 24-h temperature forecast varies between ± 1.5 °C in regions influenced by atmospheric aerosol. The biases depend on the properties of aerosol, the underlying land surface, and aerosol–cloud interactions over oceans. It is also revealed that forecast errors are rapidly magnified over time in regions featuring high aerosol loadings. Our study provides direct "observational" evidence of aerosol's impacts on daily weather forecast, and bridges the gaps between the weather forecast and climate science regarding the understanding of the impact of atmospheric aerosol.

1. Introduction

Numerical weather prediction (NWP) models are run every day at major operational weather forecast centers; they are essential for everyday life and have become a paramount tool for quantitative weather prediction worldwide [1–4]. The basic concept of NWP is to solve a complex set of mathematical equations that express the atmospheric dynamics and conservation laws including mass, momentum and energy [5]. In NWP models, a set of partial differential equations is integrated forward to obtain future atmospheric states, primarily using supercomputers nowadays. Over the past half-century, NWP models have witnessed substantial progresses leading to increasing weather forecast skill [6,7]. These advances could be attributed to the steady accumulation of scientific knowledge, particularly the understandings of key processes along with their numerical parameterization and solution, and to fast technology development in both data acquisition and data assimilation [2,7].

Atmospheric aerosol, consisting of light-absorbing components like black carbon and scattering components like sulfate, is originated from primary anthropogenic and natural emissions as well as formed via secondary chemical transformations. Aerosol poses perturbations on weather and climate directly through scattering and absorbing radiation and indirectly by modifying microphysical properties of clouds, thereby exerting a cooling or heating effect on the planet [8]. Case studies have shown that aerosol is one of the important factors that may influence weather forecast [9,10]. For instance, anthropogenic aerosol may reduce the amount of sunlight reaching the ground and thus tend to cause local cooling in densely populated regions such as China and India [11]. Biomass-burning aerosol containing a large amount of light-absorbing black carbon decreases solar irradiance reaching the Earth's surface while heating the surrounding air, thus modifying the atmospheric temperature stratification [12–14]. Saharan and Asian dust aerosol probably perturbs radiation balance or serves as ice nuclei, and hence plays an important role in temperature stratification and precipitation processes [15,16].

In climate models, aerosol has already been well acknowledged as one of the largest sources of uncertainty [17–21]. However, the great importance of the seamless integrated chemistry-meteorology modeling has been less considered in the NWP application than the climate community traditionally [9,22,23], and most current operational NWP models rarely resolve the aerosol processes explicitly [1,9]. In general NWP applications,

* Corresponding author.
E-mail address: dingaj@nju.edu.cn (A. Ding).

https://doi.org/10.1016/j.scib.2021.05.009
2095-9273/

climatological aerosol with coarse spatiotemporal resolutions is usually applied for a low computational complexity. However, unlike greenhouse gases, aerosol is a climate forcer featuring great spatial heterogeneity and erratic fluctuation, and hence climatological approximation is not capable of well representing time-varying impacts of aerosol on meteorology. In addition to the expensive computational cost of integrated chemistry-meteorology modeling, the main causes for less sophisticated treatment of aerosol also include that operational NWP models have gained a much better performance owning to the rapid progress in data assimilation, which are considered to potentially fill the gaps of some missing processes like aerosol [1,22,24]. Here, by conducting an observation minus forecast (OMF) analysis with 3-year daily National Centers for Environmental Prediction (NCEP) Global Forecast System (GFS) data during 2016–2018, we found significant bias and expanding forecast errors in the daily forecast of lower-tropospheric air temperature in regions influenced by anthropogenic or natural aerosol, indicating that aerosol is an important but neglected driver biasing daily weather prediction.

2. Materials and methods

2.1. Radiosonde observations

The Integrated Global Radiosonde Archive (IGRA) is a radiosonde dataset of the National Climatic Data Center (NCDC), and consists of radiosonde and pilot balloon observations at over 2700 globally distributed stations [25]. The earliest data date back to 1905, and recent data become available in near real time. This dataset is well quality-assured to a high standard using quality assurance algorithms that check for formatting problems, physically implausible values, internal inconsistencies among variables, runs of values across soundings and levels, climatological outliers, and temporal and vertical inconsistencies in air temperature. Observations are available at standard and variable pressure levels, fixed- and variable-height wind levels, and at the surface and tropopause. The mandatory pressure levels for the measurements are 1000, 925, 850, and 700 hPa for the lower troposphere.

2.2. Global forecast and analysis data

The NCEP operational GFS has applied at a fine resolution of ~13 km since 2015, and the analysis and forecast product on a $0.25^\circ \times 0.25^\circ$ global latitude–longitude grid is openly accessible. The analysis uses myriad observations at specific locations on an irregular grid to produce a representation of the atmospheric state over the GFS model grid, which has included statistical measures of both the variability of the measurements and of the atmosphere itself [24,25]. Since the year of 2012, the global data assimilation system (GDAS) has transitioned to a 3D-Var-based ensemble-variational hybrid data-assimilation system. Existing studies have shown that each data assimilation cycle in the GFS generally incorporates more than 25,000 radiosonde observations, which has been indicated to most significantly impact the analysis accuracy, particularly for air temperature [26]. By using the analysis as the initial conditions, GFS physical forecast models then propagate an atmospheric state forward in time. The global data assimilation and forecasts are made four times daily at 0000, 0600, 1200 and 1800 UTC. Correspondingly, temperature forecast biases are derived from forecast and analysis data four times per day during 2016–2018. On a daily basis, temperature forecast biases can be analyzed in detail with other influencing factors like cloud cover and aerosol. Monthly temperature forecast biases are then calculated from the daily forecast biases.

2.3. Modeling the impact of aerosol on meteorology

To quantitatively understand the impact of atmospheric aerosol on air temperature in highly polluted regions, we conduct chemistry-meteorology online-coupled modelling using the Weather Research and Forecasting coupled with chemistry model (WRF-Chem). The model has been widely used to evaluate radiative impacts of aerosol, and the model settings were detailed in our previous studies [27,28]. In the present study, the model domain covered East Asia and its surrounding areas due to severe aerosol pollution in China and India. The simulation is conducted for the entire month of June 2018. The initial and boundary conditions of the meteorological fields are driven by the 6-h NCEP global final analysis data. Both natural and anthropogenic emissions are included. Anthropogenic emissions are obtained from the Emission Database for Global Atmospheric Research (EDGAR) database [29], which provides the emission intensity of main gaseous and particulate pollutants like sulfur dioxides, nitrogen oxides, volatile organic compounds as well as carbonaceous and inorganic aerosol. Given that dust emissions are highly dependent on meteorological conditions, the emission rate of dust aerosol is calculated online based on the GOCART emission scheme [30]. Key parameterization options include the Yonsei University scheme to parameterize boundary layer processes, the Noah land surface scheme for describing land–atmosphere interactions, the Lin microphysics scheme with the Grell cumulus parameterization for reproducing the cloud and precipitation processes, and the RRTMG short- and long-wave radiation scheme. In the WRF-Chem simulations, the aerosol compositions include sulfate, nitrate, ammonium, black carbon, organic matter and mineral dust. Carbon-Bond photochemical mechanism combined with the Model for Simulating Aerosol Interactions and Chemistry (MOSAIC) aerosol module is applied; thus, both primary emissions and secondary formation via chemical transformation are considered in the aerosol simulation. The prognostic aerosol is coupled with both short- and long-wave radiation transfer modules and microphysics modules. Two parallel numerical experiments are performed: one with aerosol perturbations on meteorology and the other without.

2.4. Other observations and dataset

The Monitoring Atmospheric Composition and Climate and megacity Zoom for the Environment (MACCity) emission dataset is applied for demonstrating anthropogenic emissions, and emission intensity from biomass burning is obtained from the Global Fire Emissions Database (GFEDv4) [31]. The aerosol optical depth (AOD) is provided by Multi-angle Imaging SpectroRadiometer (MISR) product [32]. The vertical profiles of aerosol and cloud are derived from the Cloud-Aerosol Lidar and Infrared Pathfinder Satellite Observations (CALIPSO) aerosol product [33]. Land cover and snow information are derived from Moderate Resolution Imaging Spectroradiometer (MODIS) land cover (MCD12C1) and snow retrievals (MYD10) [34,35]. The shortwave radiation flux is obtained from Clouds and the Earth's Radiant Energy System (CERES) surface data product [36].

3. Results

3.1. Global atmospheric aerosol and temperature forecast bias

The OMF analysis provides unique insights into the potential influences from those processes that have not been considered or well presented in the models, particularly the time-varied influences [13,37–39]. Using the daily GDAS analysis and radiosonde data as "observations", respectively, in comparison with NCEP

GFS forecast, we calculate the 3-year averaged global distribution of OMF biases in predicted 24-h lower-tropospheric air temperature (T_{bias}), as shown Fig. 1a. Here we chose 24-h products for the OMF analysis because the 24-h forecast significantly influences human daily life and features smaller forecast error from various physical processes in the NWP than medium-range forecasts. We mainly focused on 925 hPa as this layer usually represents the upper boundary layer and the base of clouds, where air pollutants may influence the boundary dynamics and precipitation [10,13,14]. It shows that, despite great advances in NWP models and high-performance computing as well as comprehensive observing systems, current NWP models are still subject to notable forecast biases. A well-organized global distribution of strong bias could be clearly identified from region to region. For example, strong negative temperature biases exist in central-southern Africa, Amazon, northern India and eastern China, and positive biases are over the southern Oceans in the high latitudes of the Southern Hemisphere, the northern Atlantic, Siberia and eastern United States (US) [11,21,40]. From a global perspective, the positive and negative biases (with monthly means up to ±1.5 °C) are almost balanced with each other, resulting in an overall small global mean bias of –0.03 °C (Fig. 1a).

To further explore the impact of aerosol, the probability density distributions of the daily temperature forecast bias under different AOD conditions are analyzed. As clearly shown in Fig. S1 (online), the probability of $|T_{bias}|$ less than 0.5 ℃ is 96.1% under clean conditions, which is substantially higher than the corresponding probability value of 76.6% under polluted conditions. Atmospheric aerosol is an obvious factor that biases the temperature forecast. Although model uncertainties in other physical processes might be an important contributor to temperature forecast bias under specific conditions, overall, there exists much more significant bias in temperature forecast under higher aerosol loading across the globe. Such a tendency also holds true over spatial scales. The spatial pattern of OMF biases coincides with the overall distribution of aerosol (Fig. 1b), which can be well explained by various types of aerosol as a dominant contributor to the AOD, such as sea salt, mineral dust, and carbonaceous aerosol from biomass burning or fossil fuel combustions in different regions, as shown in Fig. S2 (online) [41]. The forecast biases in temperature exist mainly in the lower-middle troposphere, with signals gradually decreasing with increasing altitude (see Fig. S1 online). Fig. 1a also shows that the radiosonde–GFS bias has a consistent spatial distribution but stronger signals in comparison with GDAS–GFS bias (Figs. 1 and S3a online). Such kind of difference mainly exists below 850 hPa with more impact from aerosol (Fig. S3b, c online). Hence, even with a large number of assimilated observations, the model could only overcome about half of the bias for the analysis/reanalysis data in the lower troposphere. It is noteworthy that when data assimilation was only applied for the initial conditions, it was less effective in reducing the potential impacts of aerosol in operational weather forecasting.

3.2. Air temperature forecast bias in typical polluted regions

The maximum and minimum monthly averaged OMF T_{bias} in Figs. 2 and S4 (online) show distinct differences between regions. Most of the positive biases exist in spring and winter. The boreal Eurasian continent (i.e., from Europe to Siberia) features a particularly strong positive bias (with a regional average of up to 0.7 °C), followed by the positive biases of the coastal eastern US and the southern Oceans (Figs. 2a, c, d and S5 online). For the minimum

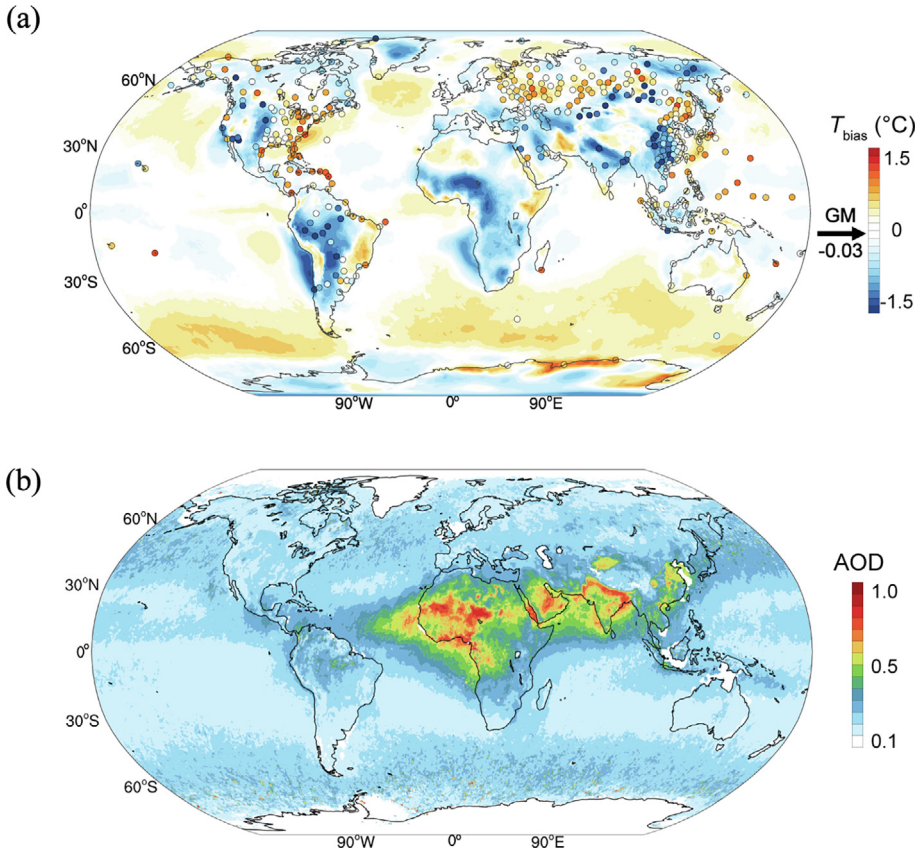

Fig. 1. Global distribution of air temperature forecast bias and aerosol. (a) 925 hPa observation minus forecast (OMF) air temperature bias (T_{bias}) for the GFS 24-h forecast compared with the GDAS analysis (GDAS-GFS, shaded contour) and radiosonde observations (radiosonde-GFS, circles) during 2016–2018. The global mean forecast bias (GM) is labeled on the color bar. (b) The global distribution of the averaged MISR aerosol optical depth (AOD) during 2016–2018.

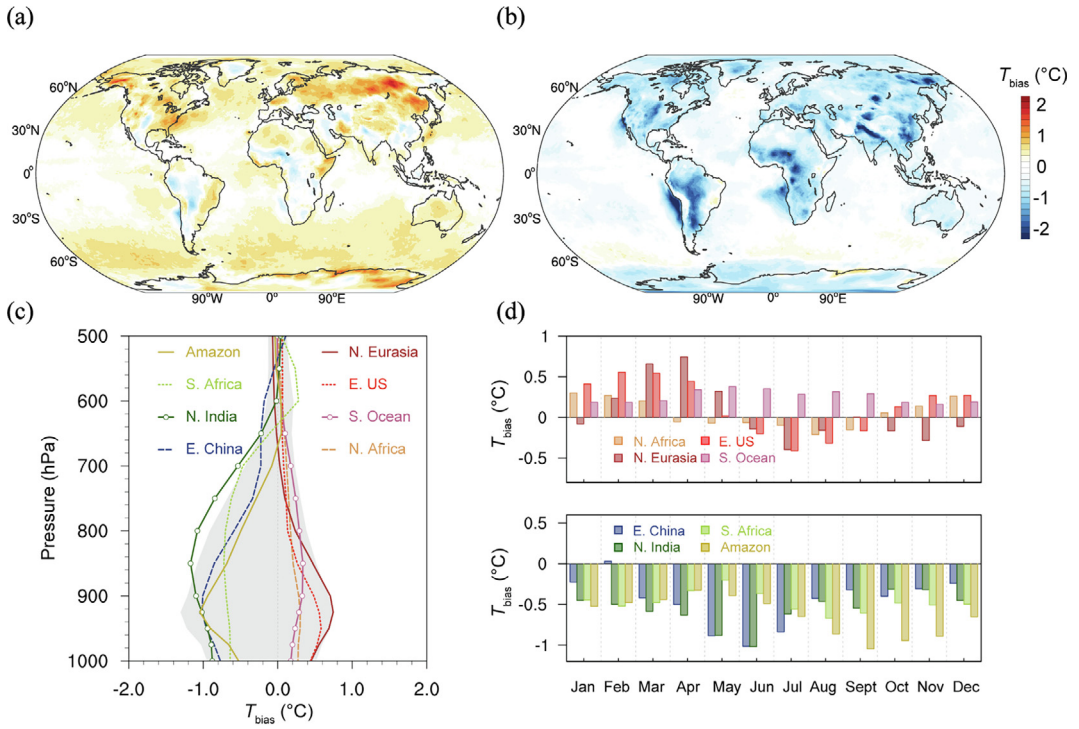

Fig. 2. Regional difference in positive and negative monthly-averaged air-temperature bias. (a, b) Maximum and minimum monthly-mean OMF T_{bias} (GDAS-GFS) in 24-h air temperature forecast at 925 hPa. (c) Vertical profiles of 24-h OMF T_{bias} (GDAS-GFS) for typical regions subject to different forcing of aerosol, including Amazon, southern and northern Africa (S. and N. Africa), northern India (N. India), eastern China (E. China), northern Eurasia (N. Eurasia), eastern US (E. US) and southern Ocean (S. Ocean). These regions are defined in Fig. S5. (d) Seasonal variations of regional-averaged OMF T_{bias} (GDAS-GFS) in typical regions.

monthly averaged OMF T_{bias}, central-southern Africa and southeastern Atlantic, and Amazon exhibit stronger negative biases (up to −1.5 °C), followed by northern India and eastern China (Figs. 2b and S5 online).

The vertical and seasonal distributions of air temperature bias averaged over the main regions suggest distinct roles of different types of aerosol in modifying air temperature, as demonstrated in Figs. 2c, d and S2 (online). Fig. 3 presents more detailed evidence from the OMF analysis and CALIPSO retrievals regarding the impact of aerosol on the air-temperature forecast bias for Asia. Consistent with the previous study [27], the well-organized and strong negative OMF value (Fig. 3a) is quite clear in northern India and eastern China in June, the month with minimum negative OMF values (Fig. 2d). The OMF T_{bias} generally coincides with the horizontal distribution of AOD contributed by anthropogenic emissions [41–43] and also show an overall inverse relation vertically (Fig. 3c). Simulations based on regional chemistry-meteorology online coupled model also indicate that aerosol could lead to a ~1 °C decrease of near-surface air temperature in emission-intensive areas like eastern China and northern India (Fig. 3b). However, coastal eastern US is characterized by significantly high positive OMF values correlated to aerosol loadings in March, when biomass burning is active in both Central America and Southeastern US [44]. The fire smoke containing light-absorbing aerosol may result in the opposite effect on the lower-tropospheric air temperature over the land in southeastern US and the downwind Atlantic Ocean (Fig. S6 online).

In addition to the two typical regions, the impacts of aerosol on the lower tropospheric temperature forecast bias in the NWP are also evident in some other regions in Fig. 2. For example, a combined effect of smoke over snow cover may well explain the significantly high positive OMF values in boreal Eurasian continent in April [45,46] (Fig. S7 online). The warming due to both short- and long-wave radiative heating of dust aerosol over regions downwind both the Sahara and Taklamakan deserts (Fig. S8 online) and dimming effect of smoke aerosol from intensive biomass burning and a possible interaction with clouds in Africa (Fig. S9 online) in typical seasons, which have been extensively studied [43,47–49], could be well identified by the OMF analysis. For the Amazon region, a minimum negative OMF bias in August and September (Fig. 2) indicates a possible impact from smoke-induced cloud condensation nuclei (CCN) increment, even though the averaged AOD is not as high as other polluted regions [50] (Figs. 1 and 2).

Although our results are generally consistent with previous works on aerosol radiative forcing and their impact on regional climate in these regions, it should be noted that the OMF analysis here is derived from numerical weather forecast rather than simulations with explicit descriptions of aerosol and meteorology-chemistry coupling. These results demonstrate that the OMF analysis, which is conducted for different regions and different seasons using a unified method, can provide unique insights into the impact from the missing processes (e.g., aerosol) on weather forecast and regional climate from a global perspective. However, more detailed and quantitative understandings of how different aerosols and other plausible factors, e.g., soil type and soil moisture, surface vegetation types, surface evapotranspiration, snow and ice cover, urban heat island configurations, and other boundary layer processes, influence the lower-tropospheric air temperature in different regions still require further modeling efforts.

3.3. Impacts of cloud cover and the underlying surface

As mentioned above, many factors, including cloud and the underlying surface, could influence the bias of weather prediction [51]. Here we further explore the impact from aerosol in comparison with cloud cover and surface albedo based on the OMF analysis. Because the impact of aerosol on air temperature, from both direct and indirect effects, all depends on solar radiation, aerosol

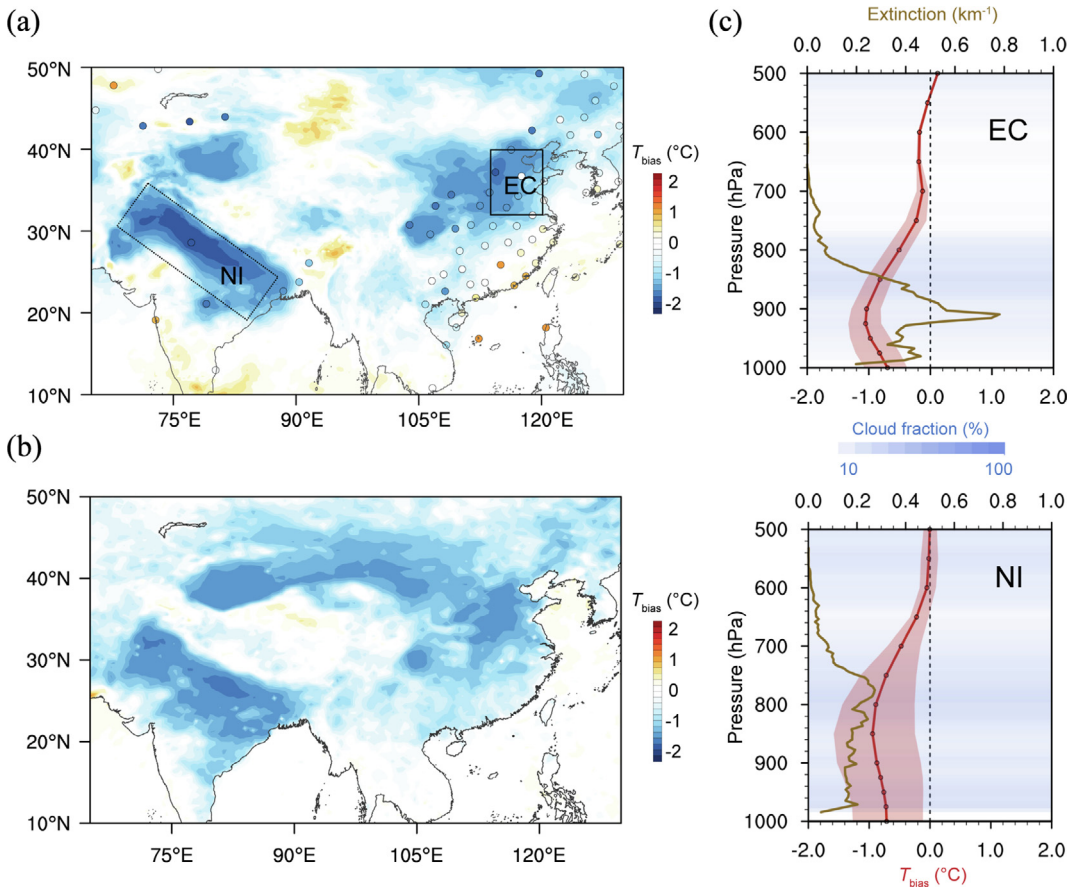

Fig. 3. Temperature response to aerosol in highly-polluted regions of India and China. (a) Spatial distribution of OMF T_{bias} between GFS 24-h forecast and GDAS analysis at 925 hPa in Asia in June. (b) Simulated aerosol's impact on 925-hPa temperature in June based on WRF-Chem model. (c) Vertical profiles of temperature forecast bias, aerosol extinction and cloud fraction retrieved by CALIPSO in northern India (NI) and eastern China (EC).

optical depth (AOD) times shortwave radiation (SW) is used as a proxy (denoted as AOD × SW) to investigate the relationship of aerosol and air temperature biases as well as other relevant processes, e.g., the underlying surface and clouds, that may influence the aerosol–radiation interaction [6,19]. Fig. 4a suggests that the air-temperature bias over land is generally larger over a darker surface with small surface albedo, and *vice versa* (Fig. S10 online). These results indicate the hybrid and interlinked effects of aerosol and land-use/land cover change, which have usually been studied separately [52] and may have been misunderstood in some cases. For instance, previous studies usually attributed the OMF or observation minus reanalysis (OMR) bias to land-surface process, e.g., urbanization, alone [39,50].

Over the ocean, a warm bias exists mainly over regions with a strong wind speed (WS greater than 15 m s^{-1}) (Fig. 4c), which causes intensive emission of wind-blow sea-salt aerosol [41] (Fig. S1 online). Fig. 4c also shows that the air temperature bias from strong wind speed slightly decreases with an increasing AOD × SW proxy, indicating a change of regimes from aerosol–cloud interaction to aerosol–radiation interaction under increasing concentration of sea-salt aerosol [20,53]. In addition, Fig. 4c also reveals a slightly negative temperature bias with large error bars for low clouds over the ocean. The scatter plot of bias in the column cloud water below 500 hPa versus the air temperature bias clearly demonstrates a strong relationship for cloud top below 850 hPa, whereby an increase in cloud water is associated with a significant decrease in air temperature (Fig. 4d). In fact, the enhanced cloud water mainly exists over regions downwind of intensive biomass burning smoke like southeastern Atlantic and subtropical Asia [38,54], where the smoke-induced semi-direct effects enhance low cloud and dim the lower tropospheric temperature (Figs. 2b and S9d online). Some studies have revealed that when the absorbing aerosol from biomass burning resides above a low cloud deck over southeastern Atlantic, the absorption of sunlight by the aerosol causes a reduction in cloud-top entrainment, leading to a thickening of the cloud deck and also a negative semi-direct forcing [18,48,49]. In contrast, the cloud bias over land shows a weaker relation with air temperature bias while compared with that over the ocean (Fig. 4b). Temperature forecast biases under clear-sky and all-sky conditions over land show a comparable magnitude (Fig. S11 online), indicating a more important role of aerosol–radiation interaction over the continent. Contrary to this, temperature forecast biases tend to be amplified by the presence of clouds.

3.4. Bias magnification with prediction time

The above analysis based on 24-h NWP modeling results clearly demonstrates the impact of aerosol in modifying daily air temperature forecast over many regions across the globe. Nowadays, people usually pay attention to weather prediction with a time window for 3–5 d and even longer. Fig. 5 shows that the bias in air temperature prediction under high aerosol conditions is statistically greater than those under clean circumstance. Fast expanded forecast errors exist in the northern India and eastern China with severe haze pollution from anthropogenic fossil fuel combustion sources [14,28] (Fig. 5b), and in Africa and Amazon with intensive biomass burning [48,49] (Fig. 5c–e). A significantly higher and increasing root mean square error with forecast time is

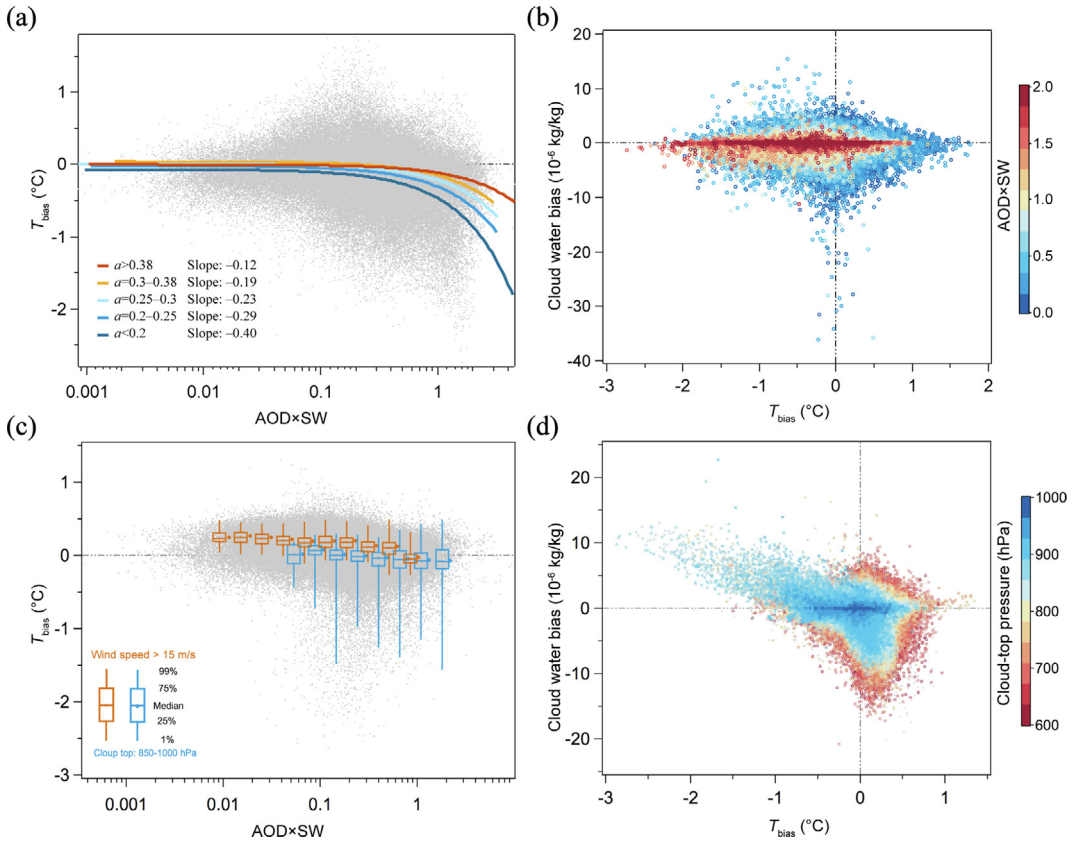

Fig. 4. Relationship of air temperature bias T_{bias} with main factors over land and sea. (a) 925-hPa OMF temperature bias (GDAS-GFS) as a function of the aerosol-radiation proxy (i.e., the aerosol optical depth multiplied by short-wave radiation (AOD × SW)) over land. Liner fittings for data with different albedo *α*. (b) OMF bias (GDAS-GFS) in column cloud water below 500 hPa as a function of OMF temperature bias at 925 hPa over land, color-coded with AOD × SW. (c) Same as (a) but for the ocean. The brown and blue box-whisker plots show data with a wind speed above 15 m s^{-1} and a cloud top below 850 hPa, respectively. (d) Same as (b) but for data over the ocean, color coded with the cloud-top pressure.

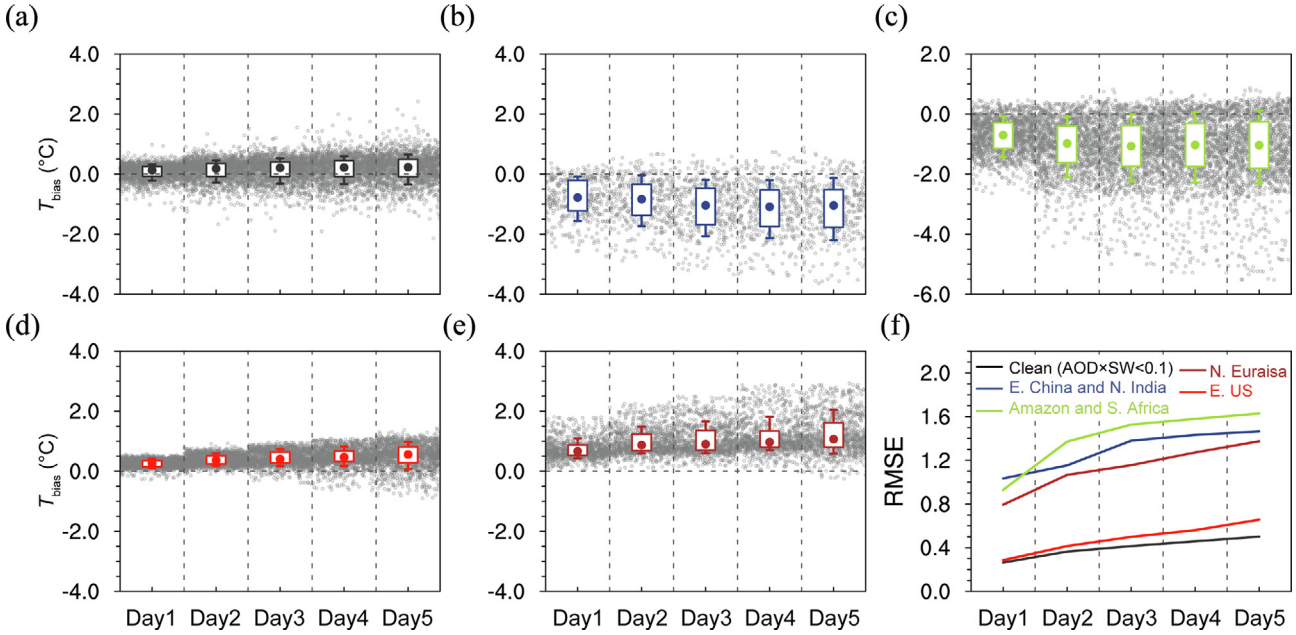

Fig. 5. Increasing biases with prediction time in high aerosol regions. 925-hPa OMF air temperature biases of 1-d to 5-d prediction in different regions. (a) Clean land area with AOD × SW less than 0.1, (b) regions with significantly high anthropogenic pollution including eastern China and northern India in June (E. China and N. India), (c) regions substantially influenced by the smoke from biomass burning, including southern Africa (S. Africa) and the Amazon in August, (d) eastern US (E. US) in February, and (e) northern Eurasia (N. Eurasia) in April. (f) Time series of root mean square error (RMSE) of air temperature forecast in the GFS in comparison to the GDAS in the same regions as (a-e). Note: we show the forecast biases at 24-h intervals of the prediction time. The grey dots in each column correspond to the same prediction time in all subplots.

demonstrated to be more substantial in regions with higher aerosol loading than regions with lower aerosol loadings (Fig. 5f). Such increasing bias in the predicted air temperature with increased forecast time was also observed globally over the main land and ocean areas (Fig. S12 online). This implies that aerosol not only biases air temperature, but also adds more uncertainty and causes poor predictability in weather forecasts in regions with high aerosol loadings. In such regions, the characterization of aerosol processes, either anthropogenic haze pollution or naturally emitted aerosol, is a key challenge for NWP models to improve the skills of multi-day weather prediction. It is also worth noting that regions with high aerosol loadings are usually characterized by dense populations (e.g., Asian countries) or fragile ecosystem/agricultural fields (e.g., arid–semi-arid regions in Africa and central Eurasia). The weaker predictability of weather forecasts in these regions is expected to exert more socioeconomic impacts on everyday life.

With respect to predictability, Fig. 5f suggests a generally linear change of biases with forecast time and Fig. S12 (online) shows that in addition to an increasing amplitude, the spatial pattern of air temperature forecast bias was less changed with forecast time. These indicate that the forecast bias is mainly caused by aerosol–radiation interaction locally and the forecast error is less propagated to downwind regions. This is good news for a practical improvement of numerical weather prediction. Since that the forecast bias generally has good correlation with aerosol under a specific underlying surface or cloud regime, the application of new technologies, like artificial intelligence [55], may help reduce the bias and improve the overall skills of the weather forecasting.

4. Discussion

In this study, we demonstrate that the current state-of-the-art NWP models are still subject to large discrepancies in forecasting tropospheric air temperature in many regions. According to the OMF analysis, available observations and model simulations, we found that the bias in air temperature forecast in many regions might be linked with different types of aerosol, despite a revolution of NWP models due to improved knowledge, fast development of high-performance computers, and massive observations available for data assimilation. The biases in air temperature forecast are different in vertical profiles and also in seasonal variations for various kinds of aerosol over different underlying surface. In general, the dimming effect of aerosol occurs in regions with high aerosol loading over land, e.g., significantly high anthropogenic aerosol in India and China and heavy smoke and dust in Africa, or regions with strong aerosol–cloud interactions, e.g., the smoky Amazon and the biomass burning-enhanced low cloud in Southern Atlantic Ocean. The warming effects of aerosol are more complex, especially in remote areas and oceans, where the effect of either the aerosol–radiation interaction or aerosol–cloud interaction might be an important contributor. The warming regions identified by the OMF analysis include the eastern US (mainly influenced by biomass burning), the boreal Eurasian continent (with smoke aerosol over the snow surface in spring), the areas downwind of the Sahara and Taklamakan deserts, and the southern oceans (linked with a possible impact from the aerosol–cloud interaction of sea salt). To minimize these biases, more measurements, including those from radiosonde observations and satellite retrievals in the lower troposphere, should be added in these regions. Considering air temperature is a principle meteorological parameter, which influences advection, convection, boundary layer dynamics and cloud formation [9,13], the aerosol-induced air temperature biases should be very crucial for the prediction of other meteorological parameters, e.g., precipitation and even circulations [13,56]. To improve the overall forecasting skills in different regions of the world with respect to the influence of aerosol, new technologies like deep learning are potentially promising means to reduce the bias. However, the long-termly ultimate solution is to develop and apply operational NWP models fully characterizing the physical and chemical processes of aerosol as well as the coupling of detailed characterization of their spatiotemporal variations.

Conflict of interest

The authors declare that they have no conflict of interest.

Acknowledgments

This work was supported by the National Natural Science Foundation of China (41725020 and 41922038). We are grateful to the National Centers for Environmental Prediction (NCEP) for making the Global Forecast System (GFS) data and global data assimilation system (GDAS) data publicly available. Maps in this article were reviewed by Ministry of Natural Resources of the People's Republic of China (GS(2021)2365).

Author contributions

Aijun Ding and Xin Huang conceived the study and led the overall scientific questions. Xin Huang performed the data analysis and modeling studies. Aijun Ding and Xin Huang wrote the paper.

Appendix A. Supplementary materials

Supplementary materials to this article can be found online at https://doi.org/10.1016/j.scib.2021.05.009.

References

[1] Bauer P, Thorpe A, Brunet G. The quiet revolution of numerical weather prediction. Nature 2015;525:47–55.
[2] Benjamin SG, Brown JM, Brunet G, et al. 100 years of progress in forecasting and NWP applications. Meteorol Monogr 2019;59:13.1–13.67.
[3] Environmental Modeling Centerof National Centers for Environmental Prediction. The GFS atmospheric model. NCEP Office Note 2003;442:14.
[4] Hollingsworth A, Engelen RJ, Textor C, et al. Toward a monitoring and forecasting system for atmospheric composition: the GEMS project. Bull Am Meteorol Soc 2008;89:1147–64.
[5] Pu Z, Kalnay E. Numerical weather prediction basics: models, numerical methods, and data assimilation. In: Duan Q, Pappenberger F, Thielen J, editors. Handbook of hydrometeorological ensemble forecasting. Berlin, Heidelberg: Springer; 2019. p. 67–97.
[6] Dudhia J. A history of mesoscale model development. Asia-Pac J Atmos Sci 2014;50:121–31.
[7] Hong S-Y, Dudhia J. Next-generation numerical weather prediction: bridging parameterization, explicit clouds, and large eddies. Bull Am Meteorol Soc 2012;93:ES6–9.
[8] Myhre G, Samset BH, Schulz M, et al. Radiative forcing of the direct aerosol effect from AeroCom Phase II simulations. Atmos Chem Phys 2013;13:1853–77.
[9] Baklanov A, Brunner D, Carmichael G, et al. Key issues for seamless integrated chemistry-meteorology modeling. Bull Am Meteorol Soc 2017;98:2285–92.
[10] Saide PE, Spak SN, Pierce RB, et al. Central American biomass burning smoke can increase tornado severity in the US. Geophys Res Lett 2015;42:956–65.
[11] Menon S, Hansen J, Nazarenko L, et al. Climate effects of black carbon aerosols in China and India. Science 2002;297:2250–3.
[12] Koren I, Vanderlei Martins J, Remer LA, et al. Smoke invigoration versus inhibition of clouds over the amazon. Science 2008;321:946–9.
[13] Ding AJ, Fu CB, Yang XQ, et al. Intense atmospheric pollution modifies weather: a case of mixed biomass burning with fossil fuel combustion pollution in eastern China. Atmos Chem Phys 2013;13:10545–54.
[14] Fan JW, Rosenfeld D, Yang Y, et al. Substantial contribution of anthropogenic air pollution to catastrophic floods in Southwest China. Geophys Res Lett 2015;42:6066–75.
[15] Creamean JM, Suski KJ, Rosenfeld D, et al. Dust and biological aerosols from the Sahara and Asia influence precipitation in the Western U.S. Science 2013;340:1572–8.

[16] Kishcha P, Alpert P, Barkan J, et al. Atmospheric response to Saharan dust deduced from ECMWF reanalysis (ERA) temperature increments. Tellus B Chem Phys Meteorol 2011;55:901–13.
[17] Carslaw KS, Lee LA, Reddington CL, et al. Large contribution of natural aerosols to uncertainty in indirect forcing. Nature 2013;503:67–71.
[18] Koch D, Del Genio AD. Black carbon semi-direct effects on cloud cover: review and synthesis. Atmos Chem Phys 2010;10:7685–96.
[19] Ramanathan V, Crutzen PJ, Kiehl JT, et al. Atmosphere: aerosols, climate, and the hydrological cycle. Science 2001;294:2119–24.
[20] Rosenfeld D, Sherwood S, Wood R, et al. Climate effects of aerosol-cloud interactions. Science 2014;343:379–80.
[21] Seinfeld JH, Bretherton C, Carslaw KS, et al. Improving our fundamental understanding of the role of aerosol-cloud interactions in the climate system. Proc Natl Acad Sci USA 2016;113:5781–90.
[22] Baklanov A, Schlunzen K, Suppan P, et al. Online coupled regional meteorology chemistry models in Europe: current status and prospects. Atmos Chem Phys 2014;14:317–98.
[23] Grell G, Baklanov A. Integrated modeling for forecasting weather and air quality: a call for fully coupled approaches. Atmos Environ 2011;45:6845–51.
[24] Whitaker JS, Hamill TM, Wei X, et al. Ensemble data assimilation with the NCEP Global Forecast System. Mon Weather Rev 2008;136:463–82.
[25] Durre I, Vose RS, Wuertz DB. Overview of the Integrated Global Radiosonde Archive. J Clim 2006;19:53–68.
[26] Kutty G, Wang XG. A comparison of the impacts of radiosonde and AMSU radiance observations in GSI based 3DEnsVar and 3DVar data assimilation systems for NCEP GFS. Adv Meteorol 2015;2015:280546.
[27] Huang X, Wang ZL, Ding AJ. Impact of aerosol-PBL Interaction on haze pollution: multiyear observational evidences in North China. Geophys Res Lett 2018;45:8596–603.
[28] Ding AJ, Huang X, Nie W, et al. Enhanced haze pollution by black carbon in megacities in China. Geophys Res Lett 2016;43:2873–9.
[29] Crippa M, Guizzardi D, Muntean M, et al. Gridded emissions of air pollutants for the period 1970–2012 within EDGAR v4.3.2. Earth Syst Sci Data 2018;10:1987–2013.
[30] Ginoux P, Chin M, Tegen I, et al. Sources and distributions of dust aerosols simulated with the GOCART model. J Geophys Res 2001;106:20255–73.
[31] van der Werf GR, Randerson JT, Giglio L, et al. Global fire emissions estimates during 1997–2016. Earth Syst Sci Data 2017;9:697–720.
[32] Diner DJ, Beckert JC, Reilly TH, et al. Multi-angle imaging spectroradiometer (MISR) instrument description and experiment overview. IEEE Trans Geosci Remote Sens 1998;36:1072–87.
[33] Omar AH, Winker DM, Kittaka C, et al. The CALIPSO automated aerosol classification and lidar ratio selection algorithm. J Atmos Ocean Technol 2009;26:1994–2014.
[34] Sulla-Menashe D, Friedl MA. User guide to collection 6 MODIS land cover (MCD12Q1 and MCD12C1) product. Sioux Falls: LP DAAC; 2018.
[35] Notarnicola C, Duguay M, Moelg N, et al. Snow cover maps from MODIS images at 250 m resolution, part 1: algorithm description. Remote Sens 2013;5:110–26.
[36] Wielicki BA, Barkstrom BR, Harrison EF, et al. Clouds and the Earth's Radiant Energy System (CERES): an earth observing system experiment. Bull Am Meteorol Soc 1996;77:853–68.
[37] Dahoui M, Isaksen L, Radnoti G. Assessing the impact of observations using observation-minus-forecast residuals. ECMWF Newsl 2017;152:27–31.
[38] Ding K, Huang X, Ding A, et al. Asian monsoon amplifies semi-direct effect of biomass burning aerosols on low cloud formation. EarthArXiv 2020. https://doi.org/10.31223/osf.io/ayvs7.
[39] Kalnay E, Cai M. Impact of urbanization and land-use change on climate. Nature 2003;425:102.
[40] Hyder P, Edwards JM, Allan RP, et al. Critical Southern Ocean climate model biases traced to atmospheric model cloud errors. Nat Commun 2018;9:1–17.
[41] Chin M, Diehl T, Dubovik O, et al. Light absorption by pollution, dust, and biomass burning aerosols: a global model study and evaluation with AERONET measurements. Ann Geophys 2009;27:3439–64.
[42] Li ZQ, Lau WKM, Ramanathan V, et al. Aerosol and monsoon climate interactions over Asia. Rev Geophys 2016;54:866–929.
[43] Yu HB, Dickinson RE, Chin M, et al. Direct radiative effect of aerosols as determined from a combination of MODIS retrievals and GOCART simulations. J Geophys Res 2004;109:D03206.
[44] Wang J, Christopher SA. Mesoscale modeling of Central American smoke transport to the United States: 2. Smoke radiative impact on regional surface energy budget and boundary layer evolution. J Geophys Res 2006;111:D14S92.
[45] Hansen J, Nazarenko L. Soot climate forcing via snow and ice albedos. Proc Natl Acad Sci USA 2004;101:423–8.
[46] Zhang RD, Wang HL, Fu Q, et al. Unraveling driving forces explaining significant reduction in satellite-inferred Arctic surface albedo since the 1980s. Proc Natl Acad Sci USA 2019;116:23947–53.
[47] Kaufman YJ, Koren I, Remer LA, et al. The effect of smoke, dust, and pollution aerosol on shallow cloud development over the Atlantic Ocean. Proc Natl Acad Sci USA 2005;102:11207–12.
[48] Lu Z, Liu XH, Zhang ZB, et al. Biomass smoke from southern Africa can significantly enhance the brightness of stratocumulus over the southeastern Atlantic Ocean. Proc Natl Acad Sci USA 2018;115:2924–9.
[49] Zuidema P, Redemann J, Haywood J, et al. Smoke and clouds above the southeast Atlantic upcoming field campaigns probe absorbing aerosol's impact on climate. Bull Am Meteorol Soc 2016;97:1131–5.
[50] Andreae MO. Correlation between cloud condensation nuclei concentration and aerosol optical thickness in remote and polluted regions. Atmos Chem Phys 2009;9:543–56.
[51] Morcrette CJ, Van Weverberg K, Ma HY, et al. Introduction to CAUSES: description of weather and climate models and their near-surface temperature errors in 5 day hindcasts near the southern great plains. J Geophys Res 2018;123:2655–83.
[52] Intergovernmental Panel on Climate Change. Climate Change 2013 – The Physical Science Basis: Working Group I Contribution to the Fifth Assessment Report of the Intergovernmental Panel on Climate Change. Cambridge: Cambridge University Press; 2014.
[53] Rosenfeld D, Zhu YN, Wang MH, et al. Aerosol-driven droplet concentrations dominate coverage and water of oceanic low-level clouds. Science 2019;363:599.
[54] Xue L, Ding A, Cooper O, et al. ENSO and Southeast Asian biomass burning modulate subtropical trans-Pacific ozone transport. Natl Sci Rev 2021;8:nwaa132.
[55] Reichstein M, Camps-Valls G, Stevens B, et al. Deep learning and process understanding for data-driven Earth system science. Nature 2019;566:195–204.
[56] Jiang MJ, Feng JQ, Li ZQ, et al. Potential influences of neglecting aerosol effects on the NCEP GFS precipitation forecast. Atmos Chem Phys 2017;17:13967–82.

Xin Huang received her Ph.D. degree from the Peking University in 2014. Since then, she has been working at the School of Atmospheric Sciences, Nanjing University. Her research mainly focuses on emission estimation, air pollution and coupled chemistry–meteorology modelling.

Aijun Ding received his Ph.D. degree in meteorology from the Nanjing University in 2004, and currently is a professor at the School of Atmospheric Sciences, Nanjing University. He has been engaged in field measurement, data analysis, and numerical modeling for air pollution and their interactions with planetary boundary layer, weather and climate.